The Astrophysical Journal, 756:188 (11pp), 2012 September 10 doi:10.1088/0004-637X/756/2/188

POSSIBLE CHANGES OF STATE AND RELEVANT TIMESCALES FOR A NEUTRON STAR IN LS I +61°303

A. Papitto[1], D. F. Torres[1,2], and N. Rea[1]
[1] Institut de Ciències de l'Espai (IEEC-CSIC) Campus UAB, Fac. de Ciències, Torre C5 parell, 2a planta, E-08193 Barcelona, Spain
[2] Institució Catalana de Recerca i Estudis Avançats (ICREA), E-08010 Barcelona, Spain
Received 2012 May 22; accepted 2012 July 17; published 2012 August 27

ABSTRACT

The properties of the short, energetic bursts recently observed from the γ-ray binary LS I +61°303 are typical of those showed by high magnetic field neutron stars (NSs) and thus provide a strong indication in favor of a NS being the compact object in the system. Here, we discuss the transitions among the states accessible to a NS in a system like LS I +61°303, such as the ejector, propeller, and accretor phases, depending on the NS spin period, magnetic field, and rate of mass captured. We show how the observed bolometric luminosity ($\gtrsim$few $\times 10^{35}$ erg s^{-1}) and its broadband spectral distribution indicate that the compact object is most probably close to the transition between working as an ejector all along its orbit and being powered by the propeller effect when it is close to the orbit periastron, in a so-called *flip-flop* state. By assessing the torques acting onto the compact object in the various states, we follow the spin evolution of the system, evaluating the time spent by the system in each of them. Even taking into account the constraint set by the observed γ-ray luminosity, we found that the total age of the system is compatible with being $\approx$5–10 kyr, comparable to the typical spin-down ages of high-field NSs. The results obtained are discussed in the context of the various evolutionary stages expected for a NS with a high-mass companion.

Key words: stars: magnetars – X-rays: binaries – X-rays: individuals (LS I +61303)

Online-only material: color figures

1. INTRODUCTION

LS I +61°303 is one the few high-mass X-ray binaries (HMXBs) discovered so far to emit the largest part of their luminosity at high energies (Hermsen et al. 1977; Gregory & Taylor 1978; Albert et al. 2006), being therefore a member of the class of γ-ray binaries. Variability of its emission, at the timescale set by the ∼26.5 day orbital period, has been found at almost all wavelengths, e.g., Albert et al. (2008), Abdo et al. (2009), Torres et al. (2010), and Zhang et al. (2010). The companion star is a massive B0Ve star, with a mass between 10 and 15 $M_\odot$, in an eccentric 26.5 day orbit (Casares et al. 2005). For the nature of the compact object in γ-ray binaries, models involving an accreting black hole (BH) launching a relativistic jet (the microquasar scenario; see, e.g., Bosch-Ramon & Khangulyan 2009, and references therein) and a rotation-powered neutron star (NS) emitting a relativistic wind of particles (see, e.g., Maraschi & Treves 1981; Dubus 2006; Sierpowska-Bartosik & Torres 2008) have been proposed.

The presence of a NS in LS I +61°303 would be definitely proven by the observation of pulsations, but deep searches in the radio (McSwain et al. 2011) and X-ray band (Rea et al. 2010b) were not successful, so far. This is not surprising, since free–free absorption easily washes out the pulses in the radio band, while the upper limit of $\approx$10% (3σ confidence level) on the pulsed fraction in X-rays could well be larger than the actual pulsed fraction of the source. However, in the past few years, a couple of energetic ($\approx 10^{37}$ erg s^{-1}), short ($\lesssim$0.3 s) bursts were detected by the *Swift* Burst Alert Telescope from a region of a few arcminutes of radius, compatible with the position of LS I +61°303 (De Pasquale et al. 2008; Barthelmy et al. 2008; Burrows et al. 2012: see Table 1 for their observed properties). The properties of the two bursts are typical of those observed in magnetars, namely, NSs for which emission is believed to be powered by their strong magnetic energy. It is probable that the bursts were emitted by LS I +61°303 itself. Otherwise, we would be witnessing the unlikely alignment, within a couple of arcminutes, of a gamma-ray binary (a population of objects for which a handful members are known) with a magnetar-like burst-emitting object (for which we know 20 sources). If the LS I +61°303 origin is accepted, any model of its multi-wavelength emission should thus provide an explanation of such bursts.

Under the common assumption of pulsars emitting their rotational energy via magnetic dipolar losses, the NS surface dipolar magnetic field can be estimated from the observed period and period derivative (Pacini 1967; Gold 1969). For the known magnetars, this usually ranges from $\sim 5 \times 10^{13}$ to 2×10^{15} G; recently, however, two sources with a lower field, $\gtrsim 7 \times 10^{12}$ G, were discovered, the emission of which is still believed to be powered by non-dipolar components of the magnetic field (Rea et al. 2010a, 2012; Turolla et al. 2011). About 20 magnetars are known to date, all being isolated pulsars with periods ranging from 0.3 to 12 s, usually young spin-down ages ranging between 0.7 and 230 kyr (again with the two exceptions reported above, which are also much older systems), and X-ray luminosities of the order of 10^{33}–10^{35} erg s^{-1} (see Mereghetti 2008; Rea & Esposito 2011 for recent reviews). Magnetars, historically divided into the two subclasses of anomalous X-ray pulsars and the soft gamma repeaters (SGRs), display a large variety of bursts and flares, with properties at variance with those observed from other compact objects such as accreting NSs or BHs. Magnetar bursts can be empirically divided into three main classes (although there is probably a continuum among them): the short bursts (∼0.01–1 s; 10^{37}–10^{40} erg s^{-1}), the intermediate bursts (∼5–50 s; 10^{40}–10^{42} erg s^{-1}), and the giant flares (∼100–500 s; 10^{43}–10^{47} erg s^{-1}).

Torres et al. (2012) have started to study how a high-field NS could cope with the multi-wavelength phenomenology of LS I +61°303. In their scenario, the NS would behave as a usual rotation-powered pulsar only when far from the companion star, whereas close to periastron, the increased pressure exerted by

Table 1
Bursts Observed by *Swift*-BAT from LS I +61°303

	Burst No. I[a]	Burst No. II[b]
Date	2008 Sep 10	2012 Feb 5
Position uncertainty	2′.1	3′
Angular separation	0′.60	1′.07
T_{100} (s)	0.31	0.044
Fluence (10^{-8} erg cm^{-2})	1.4 ± 0.6	0.58 ± 0.14
Γ	2.0 ± 0.3	3.9 ± 0.4
Luminosity (10^{37} erg s^{-1})	2.1	6.3

Notes. The positional uncertainty is given at a 90% confidence level, including also systematic uncertainties. The angular separation is calculated with respect to the position of the optical counterpart. The T_{100} duration and the fluences are estimated in the 15–50 keV band. Burst spectra were fitted by a power law with index Γ. The average luminosity is estimated by assuming a distance of 2 kpc (Frail & Hjellming 1991).
[a] Torres et al. (2012).
[b] From Burrows et al. (2012); see also http://gcn.gsfc.nasa.gov/notices_s/513505/BA/.

the matter of the Be equatorial disk would rather overcome the pulsar pressure, quenching the rotation-powered pulsar behavior. However, accretion of the matter captured would be inhibited by the quick rotation of the NS, which would then act as a propeller (Illarionov & Sunyaev 1975). Such alternation between ejector and propeller states along the orbit, which we refer to as a *flip-flop* state, was originally proposed by Gnusareva & Lipunov (1985) for NSs in close-binary orbits of high eccentricity and has already been applied to the case of LS I +61°303 by Campana et al. (1995) and Zamanov (1995).

In this paper, we delve further into this scenario, estimating the interval of spin periods at which a NS in LS I +61°303 is expected to behave either as an ejector or as a propeller and the duration of each of the states experienced by a NS in an eccentric binary system, as it spins down during its initial evolution. By taking into account the constraints set on the parameters of the system by the observed γ-ray luminosity, we also estimate the relative likelihood of observing the assumed NS in one of the different states. Results are discussed, comparing the case of an assumed high-field NS in LS I +61°303 to possibly related systems, such as rotation-powered sources in eccentric binary systems, as well as very long period HMXBs, thought to have hosted a magnetar in their early evolutionary stages.

2. SPIN EVOLUTION OF A NS

A NS evolves through different emission mechanisms during its existence, ejector, propeller, accretor, and georotator, depending on the balance between the outward pressure exerted by its electromagnetic field and the ram pressure of the surrounding matter (see, e.g., Lipunov et al. 1992; Ghosh 2007, and references therein). The electromagnetic pressure critically depends on the spin period of the NS, P, and on the strength of its dipolar magnetic field, B_1. On the other hand, if the NS has a high-mass companion, the pressure exerted by the mass lost by the latter, through a wind and possibly an equatorial disk such as in the case of a Be star, is mainly determined by the density and velocity of the outflow and by the velocity of the NS motion along the orbit. It turns out that once the NS magnetic field and the rate of mass captured by the NS, $\dot{M}_1$, are set, the state in which the NS lies is determined by its spin period, P. While at fast spin rates the NS behaves as an ejector, it is expected to become a propeller first and subsequently accrete matter on its surface as it slows down.

If the NS orbit is highly eccentric, the rate of mass captured by the NS may vary by orders of magnitude along an orbital cycle, even if the companion star is assumed to lose mass at a constant rate; along its orbit the NS may then switch from one state to the other, as with the *flip-flop*, ejector/propeller state proposed for LS I +61°303.

2.1. Ejector State

In the ejector state, a NS spinning at an angular frequency, $\Omega = 2\pi/P$, emits energy across the entire electromagnetic spectrum at the expense of its rotational energy. Spitkovsky (2006) evaluated the spin-down luminosity of a strongly magnetized oblique rotator, by solving for the dynamics of the field in the presence of conducting plasma (the so-called *force-free* limit of relativistic magnetohydrodynamics):

$$L_{\rm ej} = \left(B_1 R_1^3\right)^2 \frac{\Omega^4}{c^3}(1+\sin^2\alpha). \quad (1)$$

Here, B_1 is the dipolar magnetic field at the equator of the NS, R_1 is the NS radius, and α is the angle between the magnetic and the spin axis. The spin-down torque acting on the NS can be therefore expressed by

$$N_{\rm ej} = -\frac{L_{\rm ej}}{\Omega} = -\left(B_1 R_1^3\right)^2 \frac{\Omega^3}{c^3}(1+\sin^2\alpha). \quad (2)$$

According to the conventional pulsar models (Goldreich & Julian 1969; see Lipunov et al. 1992 for a review), a NS behaves as an ejector as long as it manages to keep the surrounding plasma from penetrating into its light cylinder, the radius of which is $R_{\rm LC} = c/\Omega$. To stop the infall of the matter captured by the gravitation of the NS before it penetrates into the light cylinder, the pressure exerted by the NS electromagnetic field must overcome the pressure of the infalling matter. Following Bondi & Hoyle (1944), the radius at which matter is captured by the gravitational field of the NS is

$$R_G = \frac{2GM_1}{v_{\rm rel}^2}, \quad (3)$$

where M_1 is the NS mass and $v_{\rm rel}$ is the velocity of the captured matter with respect to the NS. At lower radii, matter would start falling toward the NS at a velocity of the order of the free-fall value,

$$v_{\rm ff} = \sqrt{\frac{2GM_1}{r}}, \quad (4)$$

exerting a pressure

$$p_{\rm ram} \approx \rho v_{\rm ff}^2 = \frac{\dot{M}_1}{4\pi}\frac{\sqrt{2GM_1}}{r^{5/2}}, \quad (5)$$

where ρ is the gas density and the mass continuity equation was used. The pressure of the NS electromagnetic field outside the light cylinder,

$$p_{\rm ej} = \frac{L_{\rm ej}}{4\pi c r^2}, \quad (6)$$

scales less steeply with the distance than the pressure of the incoming matter inside the gravitational radius ($p_{\rm ram} \propto r^{-5/2}$); when the pressure of the captured matter evaluated at R_G overcomes the electromagnetic pressure, it is then expected to

Table 2
Scale Units Used in This Paper

Scale	Definition	Parameter
b_1	$B_1/10^{13}$ G	NS magnetic field
m_1	$M_1/1.4\ M_\odot$	NS mass
r_1	$R_1/10$ km	NS radius
$\mathcal{I}$	$I_1/10^{45}$ g cm^2	NS moment of inertia
$\dot{m}_1$	$\dot{M}_1/10^{17}$ g s^{-1}	NS mass capture rate
$\dot{m}_1^{\max}$	$\dot{M}_1{}^{\max}/10^{17}$ g s^{-1}	Max NS mass capture rate
$\dot{m}_1^{\min}$	$\dot{M}_1{}^{\min}/5\times10^{12}$ g s^{-1}	Min NS mass capture rate
b_2	$B_2/0.6$ kG	Be star magnetic field
m_2	$M_2/12.5\ M_\odot$	Be star mass
r_2	$R_2/10\ R_\odot$	Be star radius
n_2	$n/2$	Index of Be disk mass capture rate radial dependence
d_7	$d_{\rm cut}/7R_2$	Be disk cutoff size
$\dot{m}_2^p$	$\dot{M}_2^p/10^{18}$ g s^{-1}	Be star mass-loss rate
v	$v_\infty^p/10^8$ cm s^{-1}	Be star wind term. velocity

penetrate into the light cylinder as it falls inward, driving the NS out of the ejector phase as a consequence. The matter infall may be stopped in fact only by the NS magnetospheric pressure,

$$p_{\rm magn} = \left(B_1 R_1^3\right)^2 \frac{1}{8\pi r^6}. \quad (7)$$

In this case, the size of the magnetosphere is indeed defined in terms of the balance between $p_{\rm magn}$ and $p_{\rm ram}$, yielding the so-called Alfvén (or magnetic) radius,

$$R_M = \frac{\left(B_1 R_1^3\right)^{4/7}}{\dot{M}^{2/7}(2GM_1)^{1/7}}. \quad (8)$$

When the magnetosphere is able to extend up to the light-cylinder radius again (e.g., because of a decrease of the mass capture rate), the NS may then resume emitting as an ejector. The condition to recover an unscathed light cylinder [$R_M \geqslant R_{\rm LC}$, i.e., $p_{\rm ram}(R_{\rm LC}) \leqslant p_{\rm mag}(R_{\rm LC})$] is slightly different than the condition to stop the ejector mechanism [$p_{\rm ram}(R_G) \geqslant p_{\rm ej}(R_G)$]. The former condition is fulfilled at a larger NS spin period when the other relevant magnitudes are held fixed (see, e.g., the discussion in Torres et al. 2012) and can be considered more restrictive to identify when the NS abandons the ejector state. For simplicity and to be conservative, we then consider throughout this paper the equality, $R_M = R_{\rm LC}$, to define the transition both from and into the ejector state. The period at which the transition from the ejector to the propeller state takes place can be expressed in terms of the rate of mass captured by the NS, once the mass, radius, and magnetic field of the NS are fixed:

$$P_{\rm ej\rightarrow sup\ prop}(\dot{m}_1) = 0.24 b_1^{4/7}\ m_1^{-1/7}\ r_1^{12/7}\ \dot{m}_1^{-2/7}\ {\rm s}. \quad (9)$$

Here, $b_1 = (B_1/10^{13}\,{\rm G})$, $m_1 = (M_1/1.4\,M_\odot)$, $r_1 = (R_1/10{\rm km})$, and $\dot{m}_1 = (\dot{M}_1/10^{17}$ g s$^{-1})$ are the magnetic field, the mass, the radius, and the rate of mass captured by the NS, respectively, in units of the values we consider as *fiducial* in the rest of the paper (see Table 2 for a complete list of the scale units considered).

2.2. Supersonic Propeller State

When the NS stops acting as an ejector, accretion onto its surface is still inhibited by the rotation of the NS. The magnetosphere spins much faster than the infalling matter at the boundary defined by R_M, and the interchange instabilities allowing the plasma to enter into the magnetosphere are strongly suppressed (Elsner & Lamb 1977). To express the centrifugal inhibition of accretion, we introduce the corotation radius, defined as the radius at which the linear velocity of the rotating magnetosphere equals the Keplerian rate, $\Omega_K(r) = (GM_1/r^3)^{1/2}$,

$$R_{\rm co} = \left(\frac{GM_1}{\Omega^2}\right)^{1/3}, \quad (10)$$

and define the NS fastness as (Ghosh & Lamb 1979)

$$\omega_* = \frac{\Omega}{\Omega_K(R_M)} = \left(\frac{R_M}{R_{\rm co}}\right)^{3/2}. \quad (11)$$

If $R_M > R_{\rm co}$ (i.e., $\omega_* > 1$), a centrifugal barrier prevents the accretion of matter onto the NS surface, and the NS is said to lie in a *propeller* state. Illarionov & Sunyaev (1975) expressed the luminosity emitted by the NS in this state in terms of the energy needed to balance gravitational energy of infalling matter, $L_{\rm prop}^{\rm IS} = \dot{M} v_{\rm ff}^2/2$. Subsequent studies (Davies et al. 1979; Davies & Pringle 1981; Mineshige et al. 1991) showed how a quasi-static corona forms around the NS, as far as the quickly rotating magnetosphere transfers energy to the incoming matter at a rate larger than the gas cooling rate. Such a corona extends down to the radius where its pressure is balanced by the pressure of the magnetic field,[3] $R_{\rm in} \approx R_M$. At the interface between the corona and the magnetosphere the gas is shocked by the supersonic motion of the field lines, and energy is transferred to the coronal gas through turbulent or convective motions (see Wang & Robertson 1985, for a detailed treatment). Such a transfer takes place at the expense of the spin of the NS, which decelerates at a rate (see, e.g., Mineshige et al. 1991)

$$N_{\rm prop} = \frac{L_{\rm prop}}{\Omega} \approx \frac{1}{\Omega}\,\epsilon\ \times\ 4\pi R_M^2 v_t(R_M), \quad (12)$$

where ϵ is the energy density transferred by the NS during each revolution, v_t is the velocity of the turbulence developing at R_M, and $4\pi R_M^2 v_t(R_M)$ is volume of the gas perturbed by the motion of the dipolar magnetic field, assumed to be tilted with respect to the spin axis. As long as the linear velocity of the magnetosphere exceeds the sound speed at R_M (taken to be of the order of the free-fall velocity, $v_{\rm ff}$) and the energy released to the corona by the NS dominates radiative losses (see the discussion of Ikhsanov 2002, relative to wind-fed close binary systems), the propeller is considered *supersonic* and the turbulent motions take place at a velocity $v_t \simeq v_{\rm ff}$. However, there is no general consensus on the estimate of the propeller efficiency. Davies et al. (1979) and Davies & Pringle (1981) consider $\epsilon \simeq \rho v_{\rm ff}^2/2$, recovering the scaling of Illarionov & Sunyaev (1975):

$$N_{\rm prop}^{\rm IS} = -\dot{M}\sqrt{GM_1 R_M}\ \omega_*^{-1}. \quad (13)$$

On the other hand, if $\epsilon \simeq \rho(\Omega_S R_M)^2/2$ is considered, a much stronger torque is obtained (Mineshige et al. 1991; Ghosh 1995),

$$N_{\rm prop}^{G} = -\frac{1}{6}\dot{M}\sqrt{GM_1 R_M}\ \omega_*, \quad (14)$$

[3] A proper assessment of the magnetospheric boundary depends on the details of the structure of the corona. However, the ratio between $R_{\rm in}$ and R_M evaluated by a number of authors (e.g., Davies & Pringle 1981, who evaluated it as $(R_G/R_M)^{2/9}$) is of the order of 1 for the parameters considered here. In light of the large uncertainties on the plasma capture process (see Section 4), we then consider $R_{\rm in} = R_M$ to make simpler the evaluation of the torques.

where the numerical factor takes into account the degree of non-axisymmetry of the magnetosphere with respect to the spin axis (see also Wang & Robertson 1985; Illarionov & Kompaneets 1990; Bisnovatyi-Kogan 1991, who derived expressions with a similar scaling). The difference between the two estimates given by Equations (13) and (14) may be as large as $\approx 10^4$, when a NS with the fiducial parameters defined in Table 2 is rotating close to the critical period marking the transition between the ejector and the propeller state (Equation (9)), since $\omega_* \approx 100$ in that case. The discrepancy between the two propeller torques yields a significant uncertainty in the evaluation of the timescale of the NS evolution in the propeller state (see, e.g., Francischelli & Wijers 2002; Mori & Ruderman 2003). In order to be conservative when describing the evolution of LS I +61°303 in the *flip-flop* state, we consider the two estimates given above as limiting cases.

2.3. Subsonic Propeller and Onset of Accretion

As the velocity of the NS decreases and becomes comparable to the speed of sound at the inner boundary of the corona, the propeller becomes *subsonic*, with the turbulence traveling at a speed set by the NS rotation, $v_t \simeq \Omega R_M$ (Davies & Pringle 1981). We assume that such a transition takes place when $R_M \simeq R_{\rm co}$, translating into a period:

$$P_{\rm sup\ prop \rightarrow sub\ prop} = 18 b_1^{6/7}\, \dot{m}_1^{-3/7}\, m_1^{-5/7}\, r_1^{18/7}\ {\rm s}. \quad (15)$$

From Equation (12) it is deduced how the torque experienced by the NS in this stage differs by a factor $\Omega R_M / v_{\rm ff}(R_M)$ from those defined in the previous section. The rate at which energy is transferred from the NS to the surrounding corona decreases with increasing period; gas in the corona then starts to cool down, facilitating the plasma entry into the magnetosphere. A fraction of the incoming matter may then accrete down to the NS surface already in the subsonic propeller state (the so-called settling regime studied by Shakura et al. 2012). Subsequently, the cessation of any significant barrier effect is achieved when the energy released by the rotating magnetosphere to the incoming matter can be neglected with respect to the cooling of the gas; the spin period for such a transition was estimated as

$$P_{\rm sub\ prop \rightarrow acc} = 91 b_1^{16/21}\, \dot{m}_1^{-5/7}\, m_1^{-4/21}\, r_1^{16/7}\ {\rm s} \quad (16)$$

by Ikhsanov (2001), who used this expression to estimate the duration of the subsonic propeller state in wind-fed binary systems (see also Ikhsanov 2007).

3. MAGNETIC DISSIPATIVE TORQUES

The interaction between the strong magnetic field of a magnetar and the field of a low-mass, convective companion star was invoked by Pizzolato et al. (2008) to suggest how the spin period of the X-ray source 1E 161348–5055 could have been locked to the orbital period of the system, similar to what happens in polar cataclysmic variables (see e.g., Warner 2003). In such a case, it is in fact argued that a dissipative torque,

$$N_{\rm magn} \approx \frac{\mu_1 \mu_2}{d^3}, \quad (17)$$

develops as the magnetic dipole of the white dwarf, μ_1, and the magnetic field of the companion star, μ_2, interact at an orbital separation d. The magnetic field of the companion star can be either induced by the white dwarf field (e.g., Joss et al. 1979; Lamb et al. 1983; Campbell 1984) or intrinsic to the companion star (Campbell 1985; Hameury et al. 1987). The rotation of a low-mass companion star belonging to a close system ($P_{\rm orb} \approx$ few hours) is synchronized to the orbital motion by tidal forces on a relatively short timescale, $\approx 10^2$–10^3 yr, as is obtained by considering the relation given by Zahn (1977):

$$t_{\rm sync} = \frac{1}{6} \left(\frac{M_2}{M_1} \right)^2 \left(\frac{M_2 R_2^2}{L_2} \right)^{1/3} \frac{I_2}{k_2 M_2 R_2^2} \left(\frac{a}{R_2} \right)^6. \quad (18)$$

Here, M_2, R_2, L_2, and I_2 are the mass, radius, luminosity, and momentum of inertia of the non-degenerate star, k_2 is the constant of apsidal motion and is of the same order of $I_2/M_2R_2^2$ (Zahn 1977), and a is the semimajor axis of the orbit. The torque due to the interaction between the magnetic fields of the two stars then acts to bring the white dwarf to synchronicity with the orbit, as well.

The projected rotational velocity of the $\sim 12.5\, M_\odot$ Be star in LS I +61°303 was measured by Casares et al. (2005) as 113 km s^{-1}. Such a value corresponds to a spin period of $\simeq 4.5\, r_2\, \sin i$ d, where i is the inclination of the system and $r_2 = (R_2/10\ R_\odot)$ is the radius of the companion in units of 10 $R_\odot$. Plainly put, the rotation of the Be star is not locked to the orbital period of the system. This is consistent with the time needed to synchronize the spin of the non-degenerate star to the orbit of LS I +61°303 through tidal interactions with the compact object ($\approx 10^7$ yr; see Equation (18)).

However, the magnetic field of a star with the properties of the Be star in LS I +61°303 can be in principle very intense. A surface field of $\sim$0.6 kG was measured from a star of the same luminosity class (Petit et al. 2008), while even larger fields were measured from peculiar stars with spin periods lower than 1 day (see, e.g., Table 1 in Oskinova et al. 2011, and references therein). An intrinsic field of this order is larger by orders of magnitude than any field that may be induced by the NS field, and the magnetic dipole moment of the Be star, $\approx 10^{38}$ G cm^{-3}, would be much larger than the NS moment, $\approx 10^{31}$ G cm^{-3}, as well. However, in the case of a relatively wide binary such as LS I +61°303, the steep dependence of Equation (17) on the orbital separation greatly reduces the magnitude of the torque.

4. MASS CAPTURE

The rate of mass lost by a Be star such as that in LS I +61°303, $\dot{M}_2$, is given by the sum of the mass lost through a *fast* polar wind, $\dot{M}_2^p$, and a *slow* equatorial disk, $\dot{M}_2^d$ (e.g., Waters et al. 1988). According to the Bondi–Hoyle description, the mass lost by the companion star is then captured by the NS at a rate $\dot{M}_1 = \dot{M}_2\, (R_G/d)^2/4$, where R_G is the radius of gravitational capture defined by Equation (3). The estimate of $\dot{M}_1$ obtained under this approximation is thus very steeply dependent on the velocity of the captured mass with respect to the NS, $v_{\rm rel}$. The velocity of the polar, radiatively driven outflow is described by $v^p(r) \simeq v_\infty^p (1 - R_2/d)$, where v_∞^p is the polar wind terminal velocity (e.g., Lamers & Cassinelli 1999). The orbital velocity of the compact object in LS I +61°303 can be neglected with respect to the wind velocity (see Figure 13 of Torres et al. 2012), and the rate of mass captured from the polar wind is given by

$$\dot{M}_1^p = \dot{M}_2^p \frac{(GM_1)^2}{\left(v_\infty^p\right)^4 d^2} \left(1 - \frac{R_2}{d} \right)^{-4}. \quad (19)$$

In the following, we scale the rate of mass lost by the Be star and the wind terminal velocity in units of $\dot{m}_2^p = (\dot{M}_2^p/10^{18})$ g s^{-1}

and $v = (v_\infty^p/10^8$ cm s$^{-1})$, respectively, of the order of the estimates given by Waters et al. (1988).

A rapidly rotating Be star loses mass through an equatorial disk at a rate that is generally 10–100 times larger than that of the polar wind (see, e.g., Lamers & Waters 1987). By modeling the observed IR excess, Marti & Paredes (1995) estimated the equatorial disk mass-loss rate of the Be star in LS I +61°303, M_2^d, to lie between 0.25 and 2.5×10^{19} g s^{-1}. This range depends on the value of the radial velocity of the flow at the surface of the Be star, assumed to vary in the range 2–20 km s^{-1}. However, modeling the capture of mass from the equatorial disk is much more uncertain with respect to the polar wind case. In this case, for any reasonable assumption on the radial and azimuthal velocity profile of the equatorial disk matter, the orbital velocity of the compact object in LS I +61°303 cannot be ignored, as is the case when the poloidal wind is considered. Most importantly, the Bondi–Hoyle approximation yields values of the mass capture rate at the periastron of the orbit, which may be unphysically larger than the rate of mass lost by the Be star, essentially because of the low relative velocity of the disk matter in such a system ($\lesssim 10^7$ cm s^{-1}; see Figure 13 in Torres et al. 2012). Given these large uncertainties, to model the capture of mass from the equatorial disk, we parameterize with a power law its dependence on the orbital separation, d, adding a strong cutoff at a distance $d_{\rm cut}$ to reproduce a tidal truncation of the disk due to the interaction with the compact object (Okazaki et al. 2002). We thus consider

$$\dot{M}_1^d = \dot{M}_1^{\rm max} \left(\frac{d}{d_{\rm min}}\right)^{-n} \exp\left[-\left(\frac{d}{d_{\rm cut}}\right)^{10}\right]. \qquad (20)$$

Here, $\dot{M}_1^{\rm max} = \dot{M}_1^d(d_{\rm min})$ is the maximum rate of mass captured by the NS from the equatorial disk, when the NS is close to the periastron of the orbit, i.e., at an orbital separation $d_{\rm min} = a(1-e)$. In the following, we consider the eccentricity $e = 0.63 \pm 0.11$ measured by Casares et al. (2005) and compatible with the estimates of Grundstrom et al. (2007) and Aragona et al. (2009), while the semimajor axis of the orbit, a, is estimated as 6.3×10^{12} cm by using the third Kepler law for a system with an orbital period of 26.5 days and a total mass of 14 $M_\odot$. Since the disk is much denser than the polar wind, the maximum rate of mass captured by the NS, $\dot{M}_1^{\rm max}$, is equal to the rate of mass captured from the disk, $\dot{M}_1^{d,\rm max}$; in the following, we scale this value in units of $\dot{m}_1^{\rm max} = \dot{M}_1^{\rm max}/10^{17}$ g s^{-1}, which was also used by Dubus (2006). Such a value is roughly in between the estimates considered by Zamanov (1995) and Gregory & Neish (2002), $\approx 3 \times 10^{17}$ and $\approx 0.6 \times 10^{17}$ g s^{-1}, respectively. A value of the same order, $\sim 0.5 \times 10^{17}$ g s^{-1}, was also found by Romero et al. (2007) from simulations of the interaction between the equatorial disk of the Be star in LS I +61°303 and the compact object, assumed to be accreting in the case they considered. It is also worth noting how peak accretion rates up to $\sim 6 \times 10^{17}$ g s^{-1} are deduced from the X-ray luminosity observed at the peak of the outburst shown by the pulsar 4U 0115+63 (see Ferrigno et al. 2011, and references therein), which has a B0.2Ve star companion and orbital parameters ($P_{\rm orb} = 24.3$ days, $e = 0.34$) similar to those of LS I +61°303. The index of the power law n of Equation (20) is varied between 1 and 3, to qualitatively reproduce the dependence of the mass capture rate on the distance found by the simulations of Romero et al. (2007), and in particular the ratio in the range 10–100 between the maximum and the minimum mass capture rate in the absence of a significant cutoff (see the solid curves in the left panel of Figure 13 plotted by Torres et al. 2012). The fiducial unit of the truncation radius of the equatorial disk is set to $7R_2$, of the order of the estimates given by Grundstrom et al. (2007) on the basis of the observed equivalent width of the Hα emission line. Larger values are also reported in the literature (see, e.g., Gregory & Neish 2002, who give $d_{\rm cut} \sim 12R_2$).

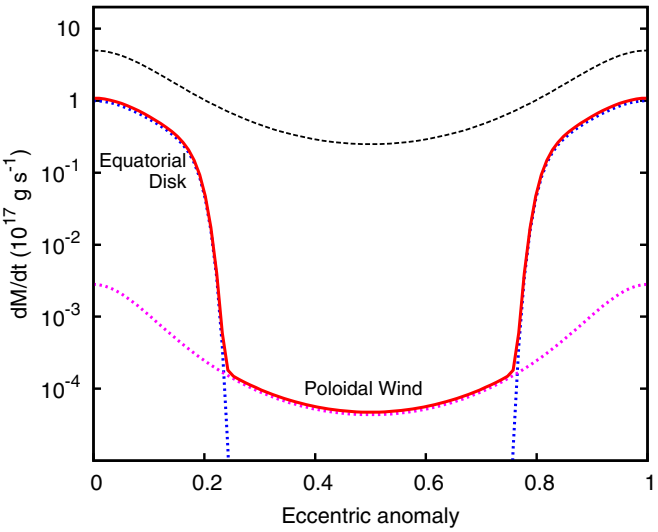

Figure 1. Rate of mass captured by a NS from the equatorial disk (blue dotted line) and the poloidal wind (magenta dotted line) emitted by the Be star in LS I +61°303, as a function of the eccentric anomaly, and for the fiducial values of the relevant parameters (see Table 2). Red solid line is the sum of these two contributions. The black dashed line shows the case of an increased Be star mass-loss rate, $\dot{m}_1^{\rm max} = 5$, and a disk cutoff beyond the maximum orbital separation, $d_{\rm cut} > a(1+e)$.

(A color version of this figure is available in the online journal.)

To evaluate the orbital dependence of the wind and disk contributions to the total rate of mass captured by the compact object, $\dot{M}_1 = \dot{M}_1^d + \dot{M}_1^p$, we use the relation $d = a(1 - e\cos\epsilon)$ to express the orbital separation in terms of the eccentric anomaly, ϵ. A red solid line shows in Figure 1 the mass capture rate as a function of ϵ, for the fiducial set of parameters. In the following, we shall also consider a mass capture rate increased by a factor of five, with an outer radius exceeding the maximum orbital separation (see black dashed line in Figure 1), in order to mimic an enhancement of the rate of mass loss of the order of that reported by Gregory et al. 1989 and Zamanov et al. 1999 to explain the observed super-orbital variability (see, e.g., Gregory 2002) with the possible expulsion of mass shells in the disk (see, e.g., Gregory & Neish 2002).

5. TIMESCALES AND CHANGES OF STATE

The time it takes for a NS to reach a period, $\bar{P}$, under the action of a spin-down torque, $N(P)$, is obtained from the integration of the equation

$$N(P) = I\dot{\Omega} = -\frac{2\pi I}{P^2}\frac{dP}{dt}, \qquad (21)$$

between the initial period, P_0, and $\bar{P}$:

$$t = -2\pi I \int_{P_0}^{\bar{P}} \frac{dP}{P^2 N(P)}. \qquad (22)$$

A NS is generally considered to spin at its birth at a period of few tens of ms, therefore spinning down as a rotation-powered

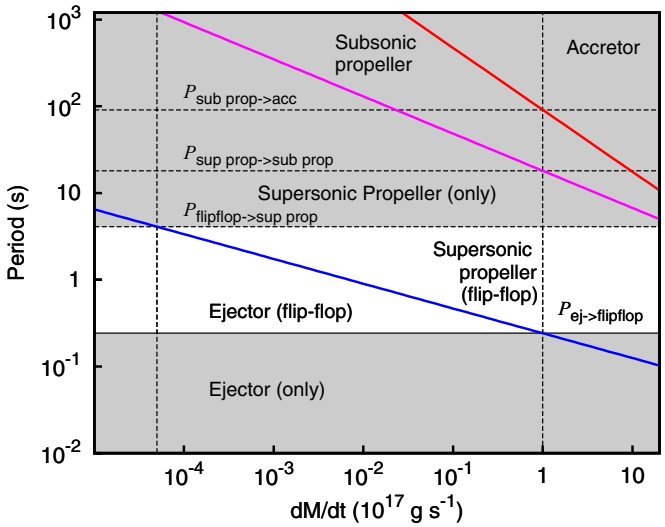

Figure 2. States accessible to a system like LS I +61°303 in the NS spin period vs. mass capture rate phase space. Solid lines mark the transitions between the ejector, supersonic propeller, subsonic propeller, and accretor states, as defined in the text (see Equations (9), (15), and (16)) and evaluated for $b_1 = 1$. Vertical dashed lines mark the minimum and the maximum capture rate experienced by the NS along its orbit, while the horizontal dashed lines indicate the values of the spin period at which transitions take place, when the relevant parameters are set equal to their fiducial values (see Table 2).

(A color version of this figure is available in the online journal.)

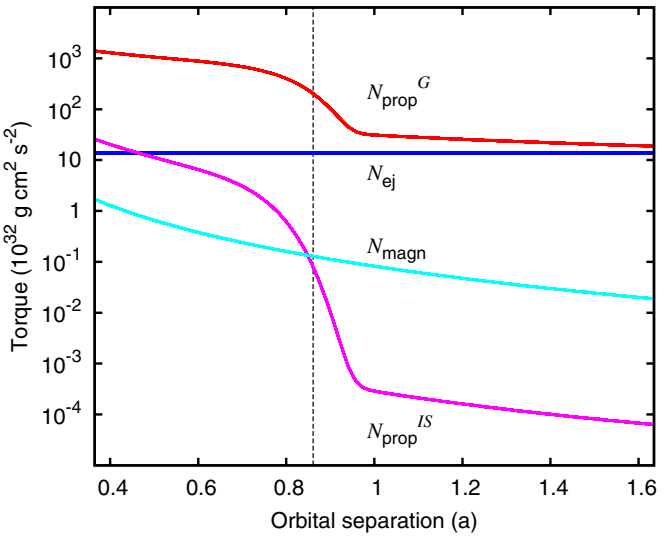

Figure 3. Propeller torque evaluated according to the two cases presented in the text (red and magenta solid curves, respectively; see Equations (13) and (14)), ejector torque (blue; see Equation (2)) and magnetic torque (cyan; see Equation (17)), plotted as a function of the orbital separation between the two stars of LS I +61°303 (expressed in units of the semimajor axis), evaluated for values of the relevant parameters set equal to the fiducial units (see Table 2), and for an example period of $P = 1$ s. Vertical dashed line marks the critical separation, $d_{\rm crit}(P = 1\ {\rm s})$, at which the system performs a transition from ejector ($d > d_{\rm crit}(P = 1\ {\rm s})$) to propeller ($d < d_{\rm crit}(P = 1\ {\rm s})$).

(A color version of this figure is available in the online journal.)

pulsar. If it belongs to a binary system such as LS I +61°303, the ejector phase will end as the pressure of the mass captured at periastron overcomes the pulsar pressure. The system then enters in the *flip-flop* state (i.e., the state at which it is in ejector phase in apastron and in supersonic propeller in periastron) when its period attains a value $P_{\rm ej\rightarrow flipflop}$. This is obtained by evaluating Equation (9) (plotted as a blue solid line in Figure 2, where the periods at which the various state transitions take place are plotted as a function of the mass capture rate, for a magnetic field $b_1 = 1$), at the maximum accretion rate experienced by the NS along its orbit, $\dot{m}_1^{\rm max}$ (rightmost vertical dashed line in Figure 2):

$$P_{\rm ej\rightarrow flipflop} = 0.24 b_1^{4/7}\, m_1^{-1/7}\, r_1^{12/7} \left(\dot{m}_1^{\rm max}\right)^{-2/7} {\rm s}. \quad (23)$$

Assuming for the moment that the magnetic field of the NS is constant, the duration of the ejector phase is found by evaluating Equation (22) between P_0 and $P_{\rm ej\rightarrow flipflop}$, with the ejector torque being described by Equation (2):

$$t_{\rm ej} = 6.3 b_1^{-6/7} \left(\dot{m}_1^{\rm max}\right)^{-4/7} m^{-2/7} r^{-18/7} \mathcal{I} (1+\sin^2\alpha)^{-1}\ {\rm kyr}, \quad (24)$$

where $\mathcal{I} = (I_1/10^{45})$ g cm^2 and I_1 is the NS moment of inertia. The value of $t_{\rm ej}$ does not significantly depend on P_0 as long as it is much smaller than $P_{\rm ej\rightarrow flipflop}$.

Evaluated at a given period, Equation (9) implicitly defines a critical value for the mass capture rate at which the NS switches from the ejector state to the propeller state (and vice versa), $\dot{M}_{\rm crit}(P)$. By using the relations given in the previous section to express $\dot{M}_1$ as a function of the orbital separation, this condition translates into a critical separation $d_{\rm crit}(P)$, defining the portion of the orbit during which the NS behaves as a propeller (for $d \leqslant d_{\rm crit}(P)$) or as an ejector (for $d > d_{\rm crit}(P)$). We then express the torque experienced by the NS during the *flip-flop* state as

$$N_{\rm ff}(d) = \begin{cases} N_{\rm ej} + N_{\rm magn} & \text{for } d > d_{\rm crit}(P) \\ N_{\rm prop} + N_{\rm magn} & \text{for } d \leqslant d_{\rm crit}(P). \end{cases}$$

Table 3
Spin Evolution Timescales

Torque	Timescale, $\Omega/\dot{\Omega}$ (kyr)
EM	$144 b_1^{-2} r_1^{-6} \mathcal{I} P^2$
IS Supersonic Propeller	$77.54 b_1^{4/7} \dot{m}_1^{-9/7} m_1^{-8/7} r_1^{12/7} \mathcal{I} P^{-2}$
G Supersonic Propeller	$1.43 b_1^{-8/7} \dot{m}_1^{-3/7} m_1^{2/7} r_1^{-24/7} \mathcal{I}$
IS Subsonic Propeller	$6.1 b_1^{-2/7} \dot{m}_1^{-6/7} m_1^{-3/7} r_1^{-6/7} \mathcal{I} P^{-1}$
G Subsonic Propeller	$0.11 b_1^{-2} m_1 r_1^{-6} \mathcal{I} P$
Magnetic Torque	$21 \times 10^3 b_1 r_1^3 b_2 r_2^3 d_6^{-3} \mathcal{I} P^{-1}$

Notes. See Table 2 for the definition of the scale units. A value of $\alpha = 45°$ was considered to estimate the electromagnetic torque. P is the NS spin period in seconds.

We summarize in Table 3 the spin evolution timescales, $\tau = \Omega/\dot{\Omega}$, implied by the torques introduced in the previous sections. The average torque experienced by the NS along one orbit is

$$\langle N_{\rm ff}\rangle = \frac{1}{P_{\rm orb}} \int_0^{P_{\rm orb}} N_{\rm ff}(t) dt = \frac{1}{P_{\rm orb}} \int_0^{2\pi} N_{\rm ff}[d(\mathcal{M})] \left|\frac{dt}{d\mathcal{M}}\right| d\mathcal{M}. \quad (25)$$

Here, $\mathcal{M}$ is mean anomaly, $|dt/d\mathcal{M}| = P_{\rm orb}/2\pi$, the relation between the mean and the eccentric anomaly is given by the Kepler's equation, $\mathcal{M} = \epsilon - e\sin\epsilon$, while the orbital separation is obtained as $d = a(1 - e\cos\epsilon)$. The magnitude and dependence on the orbital separation of the different torques introduced so far, as well as the critical distance at which the transition ejector/propeller takes place, evaluated, for example, at a period $P = 1$ s and for the fiducial parameters defined in Table 2, are plotted in Figure 3.

The NS abandons the *flip-flop* state when it reaches a period, $P_{\rm flipflop\rightarrow sup\ prop}$, such that it is in a propeller state at all points in

the orbit, even when the rate of mass capture is minimum, i.e., at apastron, $\dot{M}_{\rm crit} \simeq \dot{M}_1(d_{\rm max})$. It can be seen from Figure 1 that, as long as the equatorial disk is cut off at a distance $d_{\rm cut} < d_{\rm max}$, this value is set by the rate of mass captured by the polar wind, $\dot{M}_1^p(d_{\rm max})$. Considering a scale unit of $\dot{m}_1^{\rm min} = \dot{M}_1^{\rm min}/5 \times 10^{12}$ g s^{-1} for the minimum rate of mass capture, of the order of that expected at the apastron of the orbit if the Be star loses mass through the polar wind at a rate of 10^{18} g s^{-1}, the value of $P_{\rm flipflop\rightarrow sup\ prop}$ is found from Equation (9):

$$P_{\rm flipflop\rightarrow sup\ prop} = 4.1 b_1^{4/7} \left(\dot{m}_1^{\rm min}\right)^{-2/7} m_1^{-1/7} r_1^{12/7}\ {\rm s}. \quad (26)$$

Figure 2 shows how, for the typical values of the parameters relevant to the case of LS I +61°303, the NS leaves the *flip-flop* state well before its propeller torque becomes subsonic, and only the torques defined in Sections 2.1 and 2.2 are relevant to the evaluation of the time spent by the NS in the *flip-flop* state.

6. RESULTS AND CONSTRAINTS

6.1. The Flip-flop Phase

The total time spent in the *flip-flop* phase by a NS in LS I +61°303 is evaluated by integrating Equation (22) between $P_{\rm ej\rightarrow flipflop}$ and $P_{\rm flipflop\rightarrow sup\ prop}$. For the set of fiducial values we considered, the source stays in a *flip-flop* state when its spin period lies in the range between 0.24 and 4.1 s. The total time spent in this state crucially depends on the relation considered to express the propeller torque. Values of 25 and 282 kyr are obtained when the torques of Equations (14) and (13) are considered, respectively. Such a large discrepancy is due to the different dependence on the system fastness ω_* of the two expressions. On the other hand, the torque due to the interaction between the magnetic fields of the NS and of the companion star (see Section 3) has a negligible impact on the evaluation of the *flip-flop* timescale even if the weakest propeller torque is considered. The timescales obtained have to be compared with the interval of $\approx 10^3$ kyr it would take for a NS with the assumed fiducial values to cover the same interval of periods, only by spinning down as a rotation-powered pulsar with a constant magnetic field.

In the following, we focus on the results obtained with the stronger propeller torque, Equation (14), since it gives values that can be considered as conservative lower limits on the total time that a NS in a system like LS I +61°303 is expected to spend in the *flip-flop* phase. We plot in Figure 4 the evolutionary track of the NS spin obtained by considering the fiducial parameters defined above. The dependence of the total time spent by the system in the *flip-flop* state can be approximated as

$$t_{\rm ff} \simeq 25 b_1^{-1.1} \left(\dot{m}_1^{\rm max}/n_2\right)^{-0.3} d_7^{-1.1} \left(\dot{m}_1^{\rm min}\right)^{-0.12}\ {\rm kyr}. \quad (27)$$

Here, $d_7 = (d_{\rm cut}/7R_2)$ and $n_2 = (n/2)$. The *flip-flop* timescale depends strongly on the strength of the NS magnetic field and on the amount of mass captured by the equatorial disk of the Be star, as it is expressed by the dependence on its size, $d_{\rm cut}$, and less strongly on the maximum mass capture rate, $\dot{m}_1^{\rm max}$.

Values of the magnetic field in excess of 2×10^{14} G reduce the total *flip-flop* timescale to less than a kyr. Both the range of periods for which the NS is in the *flip-flop* state and the magnitude of the spin-down torque increase when a stronger NS magnetic field is considered, but the latter to a larger extent. The total *flip-flop* timescale also depends significantly on the amount of mass captured by the equatorial disk of the Be star. Such a time varies between ≈50 and 15 kyr when the maximum rate of mass captured varies between 10^{16} and 5×10^{17} g s^{-1}; a range of 17–36 kyr is obtained when the size of the disk cutoff takes a value between 10 and $5R_2$, while a smaller variation of ≈15% is obtained when values of n in the range 1–3 are considered.

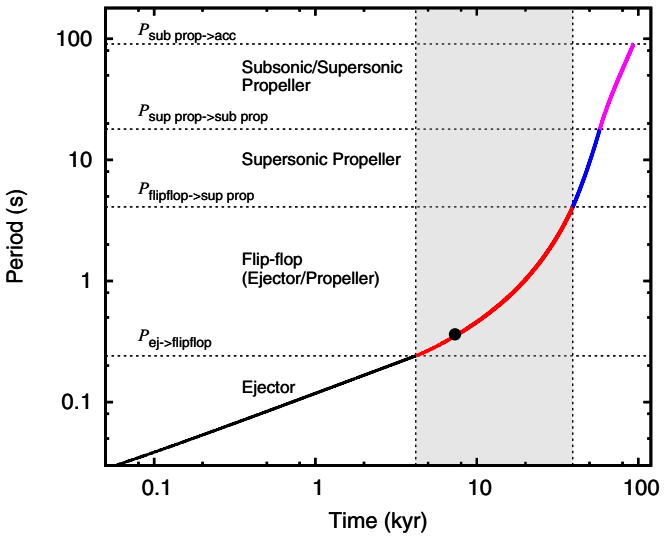

Figure 4. Evolution of the spin period of a NS in a system such as LS I +61°303, obtained considering the fiducial values of the system parameter (see Table 2). Dashed horizontal lines mark the transition among different states, while the gray shaded area marks the time interval during which the NS is expected to lie in the *flip-flop* state. The black filled circle marks the spin period at which the system emits an ejector luminosity of 5×10^{35} erg s^{-1}.

(A color version of this figure is available in the online journal.)

6.2. B-field Evolution

We have also studied the effect of the decay of the dipolar magnetic field on the total time spent by the system in the *flip-flop* state, by considering the simple relation given by Aguilera et al. (2008):

$$B_1(t) = B_0 \frac{\exp -t/\tau_O}{1 + (\tau_O/\tau_H)[1 - \exp(-t/\tau_O)]} + B_{\rm as}, \quad (28)$$

where τ_H and τ_O are the timescales for Hall and Ohm decay, set equal to 1 and 10^3 kyr, respectively, and B_0 and $B_{\rm as}$ are the initial and asymptotic value of the magnetic field, respectively. The evolutionary tracks evaluated for $B_{\rm as} = 5 \times 10^{12}$ G and a number of values of B_0 are plotted in Figure 5. For the larger initial field values we considered (50×10^{13} G), the time it takes for the NS to enter the *flip-flop* state is so short (≃0.2 kyr) with respect to the assumed value of τ_H that no significant field decay has still taken place and the timescale of the *flip-flop* state is correspondingly very short (≲kyr). On the other hand, values in excess of 10 kyr are spent by the NS in the *flip-flop* state if the initial field is $\lesssim 5 \times 10^{13}$ G.

6.3. Constraints from the Apastron Luminosity and Be-star Mass-loss Rate Variations

We plot in Figure 6 the different states (ejector, *flip-flop*, propeller) in which a NS in LS I +61°303 is expected to lie during the early stage of its evolution, depending on the values of its magnetic field and spin period; the tracks delimiting the various regions were evaluated from Equations (23) and (26), for

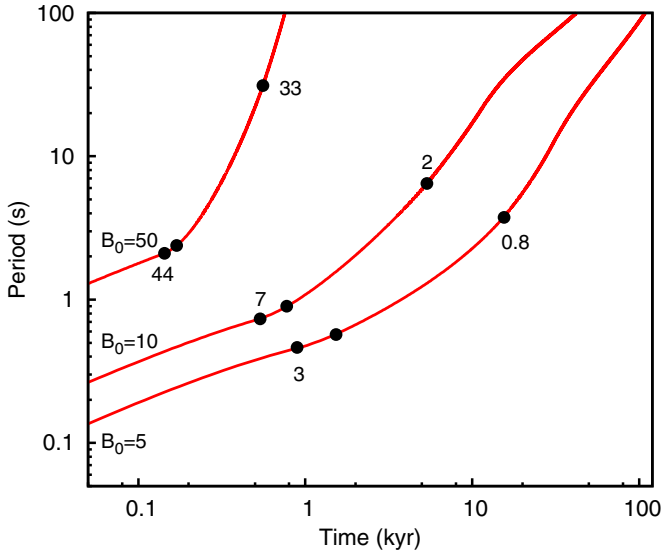

Figure 5. Evolution of the spin period as a function of the time elapsed since the NS birth with $P_0 = 0.01$ s, for values of the initial NS magnetic field equal to (from top to bottom) (50, 10, and 5) $\times 10^{13}$ G. From left to right along each track, black points refer to the ingress in the *flip-flop* state, the period at which the system emits an ejector luminosity of 5×10^{35} erg s^{-1}, and the egress from the *flip-flop* state. Numbers along each track denote the strength of the magnetic field at the ingress and egress from the *flip-flop* state, respectively, in units of 10^{13} G.

(A color version of this figure is available in the online journal.)

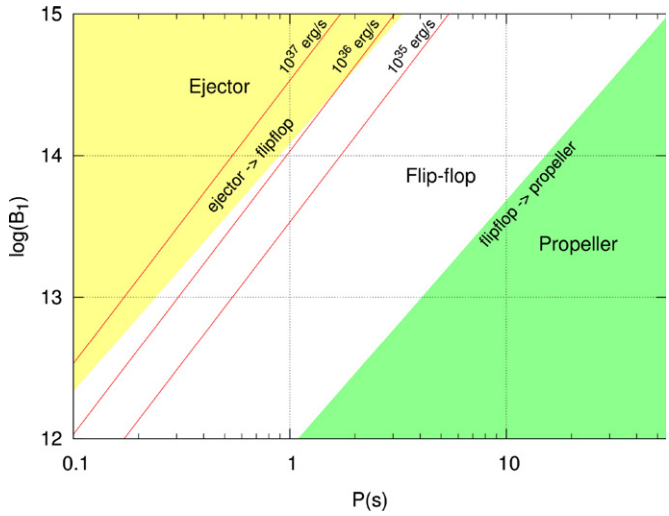

Figure 6. Ejector, *flip-flop*, and propeller states plotted in the NS magnetic field vs. spin period phase space, evaluated for a NS in LS I +61°303 and for the fiducial values adopted for the maximum and minimum mass capture rate ($\dot{m}^{\max} = 1, \dot{m}^{\min} = 1$). From top to bottom, the red solid lines mark the relation between the period and the magnetic field of the NS when the ejector luminosity is 10^{37}, 10^{36}, and 10^{35} erg s^{-1}, respectively, and the magnetic offset angle is $\alpha = 45°$.

(A color version of this figure is available in the online journal.)

fiducial units of the maximum and the minimum mass capture rate.

A relevant constraint on the possible position of LS I +61°303 in such a magnetic field versus period diagram can be drawn on the basis of the flux observed when the NS is close to apastron. According to the simplest *flip-flop* scenario discussed (i.e., not considering the possible effect of a relativistic wind on the spin-down of a magnetar, discussed by Harding et al. 1999), when in the apastron region the NS is powered by the ejector mechanism, its luminosity cannot exceed the value given by Equation (2). By evaluating such a relation for $\alpha = 45°$ and an ejector luminosity of 10^{37}, 10^{36}, and 10^{35} erg s^{-1}, the tracks plotted as red solid lines in Figure 6 are obtained.

Excluding the contribution of the bright Be star, the broad-band spectral energy distribution of LS I +61°303 peaks in the MeV–GeV band (see, e.g., Figure 6 in Chernyakova et al. 2006; Figure 2 in Gupta & Böttcher 2006, and references therein). The 0.1–300 GeV flux observed by *Fermi* Large Area Telescope when the NS is at apastron was recently estimated by Hadasch et al. (2012) as $5.1(3) \times 10^{-10}$ erg cm^{-2} s^{-1}, corresponding to a luminosity of $\sim 2.5 \times 10^{35}\ d_2^2$ erg s^{-1}, where d_2 is the distance to the source in units of 2 kpc. Such a value is $\sim$20% lower than the flux observed when the compact object is close to periastron. A flux of $\sim 2 \times 10^{-10}$ was observed by COMPTEL on board the *Compton Gamma Ray Observatory*, in the 1–10 MeV band (Tavani et al. 1996), while the source is significantly dimmer in the X-ray and TeV energy bands (see, e.g., Hadasch et al. 2012, and references therein).

If such luminosities are ejector-only generated, the spin-down power of the NS must lie in a range between few $\times 10^{35}$ and few $\times 10^{37}$ erg s^{-1} (see, e.g., the discussion of Zabalza et al. 2011, who considered an efficiency of spin-down to γ-ray luminosity conversion of $0.034(L_{\rm ej}/10^{36}\ {\rm erg\ s^{-1}})^{-1/2}$, following Abdo et al. 2010); the lower end of this interval is obtained when the emission is beamed in a 1 sr solid angle, while the higher values correspond to more isotropic pulsar beaming models. It is then clear how a pulsar with such an ejector luminosity is unlikely to lie to the right of the red line labeled as 10^{35} in Figure 6, as well as to the left of the line labeled as 10^{37}. Even recalling how the displacement of the tracks plotted in Figure 6 depends on the exact values of unknown parameters, such as the maximum rate of mass captured by the NS, as well as on the assumed ejector braking law and details on the ejector/propeller transition, the relatively large gamma-ray luminosity indicates that the NS must be young and close to the transition between the ejector phase and the *flip-flop* state.

Thus, if the source lies in a *flip-flop* state, its period must be close to the value it had at the beginning of such a phase, i.e., that given by Equation (23). This obviously reduces the time spent in the *flip-flop* state before reaching a period corresponding to a certain ejector luminosity (for a given magnetic field), with respect to that given by Equation (27). For the case of a maximum mass capture rate of $\dot{m}_1^{\max} = 1$ and a magnetic field $b_1 = 1$, the time spent in such a state before spinning down to a period corresponding to an ejector luminosity of 5×10^{35} erg s^{-1} is 3.1 kyr. By considering larger values of the ejector luminosity, the range of periods for which the NS is in the *flip-flop* phase further reduces (see Figure 6); a timescale of 1.8 kyr is obtained for an ejector luminosity of 10^{36} erg s^{-1}, while extremely small values, $\lesssim$0.1 kyr, are obtained if $L_{\rm ej} \gtrsim 2.5 \times 10^{36}$ erg s^{-1}. From Figure 6 it is also clear that the interval of periods for which the ejector luminosity deduced from the observed γ-ray flux is compatible with a *flip-flopping* behavior increases for lower magnetic fields and larger maximum mass accretion rates, with respect to the fiducial values considered.

Alternatively, the luminosity observed when the source is close to the apastron has been interpreted as powered by the propeller emission (e.g., Bednarek 2009). In such a case LS I +61°303 would lie at the right of the *flip-flop*/propeller transition (green area of Figure 6). However, even considering the stronger propeller torque introduced, Equation (14), the

expected luminosity is

$$L_{\rm prop} = \Omega N^{G}_{\rm prop} \simeq 0.9 \times 10^{36} b_1^{8/7}\, \dot{m}_1^{3/7}\, r_1^{24/7}\, m_1^{-2/7}\, P^{-2}\ {\rm erg\ s^{-1}}, \quad (29)$$

where P is the NS spin period in seconds. Such a luminosity is then compatible with the luminosity observed from the system when the NS is close to periastron (i.e., for $\dot{m}_1 \simeq 1$), if the period is $\lesssim$1 s, i.e., if the system is close to the transition between the ejector and the *flip-flop* phase. On the other hand, if the spin period is $\gtrsim$4 s, as is implied by the assumption that the source is always in the propeller state, such an effect is barely capable to power the observed emission close to periastron ($\dot{m}_1 \simeq 1$), for a NS magnetic field $\gtrsim 10^{14}$ G (i.e., $b_1 \gtrsim 10$). Close to apastron instead, the rate of mass capture is much lower, $\dot{m} \sim 10^{-4}$, and the propeller falls short by ∼two orders of magnitude in accounting for the observed γ-ray luminosity (but see below).

While the timescales derived so far do not depend much on the value of the minimum mass capture rate, $\dot{m}_1^{\rm min}$, this parameter plays a major role in determining the state of the NS at orbital phases close to apastron and therefore the value of the period at which the system abandons the *flip-flop* state (i.e., the location of the track labeled as *flip-flop*/propeller in Figure 6). In particular, an increase of the rate of mass captured by the NS, possibly caused by an increase of the rate of mass lost by the Be star and/or by a growth of the size equatorial disk, may bring the system out of the *flip-flop* state. The magnitude of the variation of the mass capture rate needed to determine such a transition obviously depends on the initial location of the source in a diagram like that of Figure 6. If the source lies close to the *flip-flop*/propeller transition, a variation by a factor of a few of the mass capture rate at apastron, owing, for instance, to an enhancement of the rate of mass lost by the Be star through its polar wind, is sufficient to inhibit the ejector emission throughout the orbit. On the other hand, if the source lies close to the ejector/*flip-flop*, as is deduced from the observed γ-ray luminosity, a much larger increase of the rate of mass captured at apastron is needed to obtain such a transition. This is, in principle, feasible if an increment of the rate of mass lost by the Be star is accompanied by an increase of the radius of the equatorial disk, so as to exceed the maximum orbital separation (see the black dashed line in Figure 1). In this framework, the super-orbital variability hinted at in TeV (Li et al. 2012) would be understood in terms of a transition toward the propeller state at all orbital phases, due to an increase of the mass-loss rate of the Be star and by an increase of its size. Such a significant increase of the mass capture rate when the NS is close to apastron would be also able to explain the observed γ-ray luminosity in terms of the propeller emission (see Equation (29)).

7. DISCUSSION

According to the conventional picture (see, e.g., Lipunov et al. 1992), a NS in a binary system evolves through ejector, propeller, and accretor states, as it spins down. While on long timescales the transition between these states is mainly set by the evolution of the spin period of the NS, on shorter timescales a key role is played by the rate at which the compact object captures the mass lost by the companion star. In particular, the large values of the ratio between the maximum and the minimum rate of mass captured by the NS achieved if the orbit is eccentric may induce state transitions along an orbital cycle, a *flip-flop* state. The range of mass capture rates spanned through an orbital cycle is even larger if the non-degenerate star is of Be class, losing mass also through a dense equatorial disk that is transversed by the NS when it is close to periastron. The existence of systems alternating states on the timescale set by the orbital period is therefore a natural consequence of the way a NS evolves.

While the observation of two magnetar-like bursts from a few-arcmin region compatible with the position of LS I +61°303 provided a strong indication in favor of a NS nature of the compact object in the system, it is unlikely that an accreting NS is hosted by LS I +61°303. Accreting NSs in Be-HMXB show in fact X-ray pulsations at a period larger than a few seconds. Moreover, their X-ray energy continuum spectrum is described by a power law with an exponential cutoff at 10–30 keV, on which cyclotron and/or iron emission features are generally superimposed (see Reig 2011, and references therein). No X-ray pulsation has been detected so far from LS I +61°303 (Rea et al. 2010b), while its X-ray spectrum is featureless and does not show a cutoff in the X-ray energy band (Chernyakova et al. 2006; Zhang et al. 2010).

On the other hand, the luminosity observed from the system is of the same order of the spin-down power liberated by the NS when its spin period is close to the critical value marking the transition from the ejector to the *flip-flop* phase. An important clue to estimate the likelihood of finding a NS in LS I +61°303 in such a phase follows from the assessment of the time spent by the system in such a state. We showed how such a timescale crucially depends on the details of the assumed propeller torque. By assuming the rotating NS to release to the incoming matter the energy needed to unbind it (see Equation (13)), or the energy effectively stored in the NS rotation (Equation (14)), largely different estimates of the evolutionary timescales are obtained. This is essentially because the rotational energy of the NS when spinning close to the ejector/propeller transition largely exceeds the gravitational energy possessed by the infalling matter, evaluated at the large magnetospheric radius implied by a strong magnetic field. Among the propeller torques considered here, the weaker yields a total duration of the *flip-flop* phase that is much larger (≈280 kyr) than the one implied by the stronger torque (≈25 kyr). Even considering the stronger propeller torque, which is favored if the system is powered by the propeller effect when the NS is close to periastron, the expected total duration of the *flip-flop* phase (see Equation (27)) is larger by a factor of ≈4 with respect to the timescale spent by the object in the pure ejector state:

$$\frac{t_{\rm ff}}{t_{\rm ej}} \approx 4\, b_1^{-0.24} \left(\dot{m}_1^{\rm max}\right)^{0.27}, \quad (30)$$

where we have made explicit only the dependence of Equations (24) and (27) on the NS magnetic field and on the maximum mass accretion rate. It is then reasonable to find the system in the *flip-flop* state. Moreover, even if it is taken into account that the system must be relatively young to emit a spin-down luminosity $\gtrsim$few × 10^{35} erg s^{-1}, the time spent by the system in the *flip-flop* phase is of a few kyr, comparable to the total duration of the previous ejector phase, and yielding an age of the system ≈5–10 kyr, of the order of typical spin-down ages of magnetars. On the other hand, a spin-down luminosity of the order of $\approx 10^{37}$ erg s^{-1} would imply a smaller age for the system, with the NS emitting as an ejector all along the orbit.

Either lying in the ejector or in the *flip-flop* state, the presence of a young NS in LS I +61°303 would make the system closely related to so-called *ante-diluvian systems* (van den

Table 4
Ante-diluvian Systems and LS I +61°303

Name	P_S (s)	P_{orb} (days)	e	B_1[a] (G)	M_2 ($M_\odot$)
J1740−3052	0.57	231.0	0.57	3.9×10^{12}	11.0–15.8
J1638−4725	0.76	1941	0.95	1.9×10^{12}	5.8–8.1
J0045−7319	0.93	51.1	0.81	2.1×10^{12}	3.9–5.3
B1259−63	0.048	1237	0.87	3.3×10^{11}	3.1–4.1
LS I +61°303	···	26.5	0.63	···	10–15

Note. [a] The magnetic field of pulsars is determined as $3.2 \times 10^{19}\ (P\dot{P})^{1/2}$ G.
References. McConnell et al. 1991; Johnston et al. 1992; Kaspi et al. 1996a; Stairs et al. 2001; Wang et al. 2004; Casares et al. 2005; Lorimer et al. 2006; we acknowledge the use of the ATNF Pulsar Catalogue, http://www.atnf.csiro.au/people/pulsar/psrcat/, Manchester et al. (2005).

Heuvel 2001), rotation-powered pulsars orbiting a high-mass companion in an eccentric orbit, considered as the progenitors of HMXBs. The properties of the four sources of this class discovered so far are listed in Table 4, together with those of LS I +61°303. We note that B1259−63 is also one of the brightest γ-ray binaries known. All these NSs have a superficial magnetic field in the range 3×10^{11}–4×10^{12} G, as derived from the observed spin-down rate. Indeed, it was early proposed that some of these systems could be found in a propeller state when the NS was close to periastron. However, the rate at which the companion star would have to lose mass in order to overcome the pulsar pressure should be much larger than expected (Campana et al. 1995; Ghosh 1995; Tavani & Arons 1997, and references therein) or observed (Kaspi et al. 1996b). Despite that a proper evaluation of the ratio defined by Equation (30) for the known *ante-diluvian* systems is far from the scope of this paper, it can be noted how the likelihood of observing a system in the pure ejector state increases when the maximum mass capture rate decreases, as is the case of at least three out of the four known *ante-diluvian* systems, lying in a much larger orbit with respect to that of LS I +61°303.

If confirmed by the discovery of pulsations, LS I +61°303 would be the first magnetar to be discovered in a binary system. The large luminosity variation shown by superfast X-ray transients on short timescales led Bozzo et al. (2008) to argue that a magnetar-like magnetic field could represent an efficient gating mechanism to make these systems rapidly switch between propeller and accreting states. That a number of accreting HMXBs should have hosted in the past a NS with a field in the magnetar range has also been claimed on the basis of their very large spin periods (e.g., 2S 0114+650 with a period of 2.7 hr; Li & van den Heuvel 1999; and 4U 2206+54 with a period of 5560 s; Finger et al. 2010; Ikhsanov & Beskrovnaya 2010; Reig et al. 2012). The spin period at which a system eventually starts accreting mass increases in fact with the strength of the magnetic field (see Equation (16) and the similar expression derived by Shakura et al. 2012 for the equilibrium period of NS in the settling regime), essentially because the value of the magnetic field sets the strength of the propeller torques that are responsible for the NS spin-down. In this context, the case of the Be/X-ray binary in the Small Magellanic Cloud, SXP 1062, with a period of 1062 s and with an estimated age of 16 kyr (Haberl et al. 2012) is noteworthy. Popov & Turolla (2012) showed how such a short age strongly points to the presence of a NS with a large initial magnetic field in the system, $\sim 10^{14}$ G, which could have spun the NS down very efficiently before the start of the accretion phase. A comparison of the age proposed for SXP 1062 with the timescales of the different propeller mechanism listed in Table 3 indicates how the faster and stronger expression for the propeller torque is probably closer to the torque effectively experienced by a NS in that system during the propeller stage. How a *strong* propeller torque, of the order of that given by Equation (14), should be possibly preferred in describing the evolution of systems like LS I +61°303 is also indicated by the ratio between the ejector and *flip-flop* timescales defined by Equation (30). If the weaker propeller torques were in place, a NS would spend a much larger time in the *flip-flop* state than in a pure ejector state, and this is not indicated by the number of systems observed in the latter state (4) with respect to the single possible case of LS I +61°303.

We finally note that, contrary to the case of SXP 1062, no association with a supernova remnant (SNR) could be made for LS I +61°303 (Frail et al. 1987). This is not entirely surprising for a source with an estimated age between 10 and 20 kyr, since such an association can be found only for a fraction 0.64 and 0.55 of the radio pulsars with such ages estimated from their electromagnetic spin-down, respectively (ATNF pulsar database; Manchester et al. 2005). Furthermore, no other Be X-ray binary has been observed embedded in an SNR, despite the relatively young age and large number of observed systems. This is most probably due to the large wind of the two progenitor massive stars, which has swept away most of the material around the binary, resulting in an underluminous (hence undetectable) SNR after the explosion.

This work was supported by the grants AYA2009-07391 and SGR2009-811, as well as the Formosa program TW2010005 and iLINK program 2011-0303. We are grateful to Rosalba Perna and Jose Pons for useful discussions.

REFERENCES

Abdo, A. A., Ackermann, M., Ajello, M., et al. 2009, ApJ, 701, L123
Abdo, A. A., Ackermann, M., Ajello, M., et al. 2010, ApJS, 187, 460
Aguilera, D. N., Pons, J. A., & Miralles, J. A. 2008, A&A, 486, 255
Albert, J., Aliu, E., Anderhub, H., et al. 2006, Science, 312, 1771
Albert, J., Aliu, E., Anderhub, H., et al. 2008, ApJ, 684, 1351
Aragona, C., McSwain, M. V., Grundstrom, E. D., et al. 2009, ApJ, 698, 514
Barthelmy, S. D., Baumgartner, W., Cummings, J., et al. 2008, GRB Coordinates Network, 8215, 1
Bednarek, W. 2009, MNRAS, 397, 1420
Bisnovatyi-Kogan, G. S. 1991, A&A, 245, 528
Bondi, H., & Hoyle, F. 1944, MNRAS, 104, 273
Bosch-Ramon, V., & Khangulyan, D. 2009, Int. J. Mod. Phys. D, 18, 347
Bozzo, E., Falanga, M., & Stella, L. 2008, ApJ, 683, 1031
Burrows, D. N., Chester, M. M., D'Elia, V., et al. 2012, GRB Coordinates Network, 12914, 1
Campana, S., Stella, L., Mereghetti, S., & Colpi, M. 1995, A&A, 297, 385
Campbell, C. G. 1984, MNRAS, 211, 69
Campbell, C. G. 1985, MNRAS, 215, 509
Casares, J., Ribas, I., Paredes, J. M., Martí, J., & Allende Prieto, C. 2005, MNRAS, 360, 1105
Chernyakova, M., Neronov, A., & Walter, R. 2006, MNRAS, 372, 1585
Davies, R. E., Fabian, A. C., & Pringle, J. E. 1979, MNRAS, 186, 779
Davies, R. E., & Pringle, J. E. 1981, MNRAS, 196, 209
De Pasquale, M., Barthelmy, S. D., Baumgartner, W. H., et al. 2008, GRB Coordinates Network, 8209, 1
Dubus, G. 2006, A&A, 456, 801
Elsner, R. F., & Lamb, F. K. 1977, ApJ, 215, 897
Ferrigno, C., Falanga, M., Bozzo, E., et al. 2011, A&A, 532, A76
Finger, M. H., Ikhsanov, N. R., Wilson-Hodge, C. A., & Patel, S. K. 2010, ApJ, 709, 1249
Frail, D. A., & Hjellming, R. M. 1991, AJ, 101, 2126
Frail, D. A., Seaquist, E. R., & Taylor, A. R. 1987, AJ, 93, 1506
Francischelli, G. J., & Wijers, R. A. M. J. 2002, arXiv:astro-ph/0205212
Ghosh, P. 1995, ApJ, 453, 411

Ghosh, P. 2007, Rotation and Accretion Powered Pulsars (Singapore: World Scientific)
Ghosh, P., & Lamb, F. K. 1979, ApJ, 234, 296
Gnusareva, V. S., & Lipunov, V. M. 1985, SvA, 29, 645
Gold, T. 1969, Nature, 221, 25
Goldreich, P., & Julian, W. H. 1969, ApJ, 157, 869
Gregory, P. C. 2002, ApJ, 575, 427
Gregory, P. C., & Neish, C. 2002, ApJ, 580, 1133
Gregory, P. C., & Taylor, A. R. 1978, Nature, 272, 704
Gregory, P. C., Xu, H.-J., Backhouse, C. J., & Reid, A. 1989, ApJ, 339, 1054
Grundstrom, E. D., Caballero-Nieves, S. M., Gies, D. R., et al. 2007, ApJ, 656, 437
Gupta, S., & Böttcher, M. 2006, ApJ, 650, L123
Haberl, F., Sturm, R., Filipović, M. D., Pietsch, W., & Crawford, E. J. 2012, A&A, 537, L1
Hadasch, D., Torres, D. F., Tanaka, T., et al. 2012, ApJ, 749, 54
Hameury, J. M., King, A. R., Lasota, J. P., & Ritter, H. 1987, ApJ, 316, 275
Harding, A. K., Contopoulos, I., & Kazanas, D. 1999, ApJ, 525, L125
Hermsen, W., Swanenburg, B. N., Bignami, G. F., et al. 1977, Nature, 269, 494
Ikhsanov, N. R. 2001, A&A, 368, L5
Ikhsanov, N. R. 2002, A&A, 381, L61
Ikhsanov, N. R. 2007, MNRAS, 375, 698
Ikhsanov, N. R., & Beskrovnaya, N. G. 2010, Astrophysics, 53, 237
Illarionov, A. F., & Kompaneets, D. A. 1990, MNRAS, 247, 219
Illarionov, A. F., & Sunyaev, R. A. 1975, A&A, 39, 185
Johnston, S., Lyne, A. G., Manchester, R. N., et al. 1992, MNRAS, 255, 401
Joss, P. C., Rappaport, S. A., & Katz, J. I. 1979, ApJ, 230, 176
Kaspi, V. M., Bailes, M., Manchester, R. N., Stappers, B. W., & Bell, J. F. 1996a, Nature, 381, 584
Kaspi, V. M., Tauris, T. M., & Manchester, R. N. 1996b, ApJ, 459, 717
Lamb, F. K., Aly, J.-J., Cook, M. C., & Lamb, D. Q. 1983, ApJ, 274, L71
Lamers, H. J. G. L. M., & Cassinelli, J. P. 1999, Introduction to Stellar Winds (Cambridge: Cambridge Univ. Press)
Lamers, H. J. G. L. M., & Waters, L. B. F. M. 1987, A&A, 182, 80
Li, J., Torres, D. F., Zhang, S., et al. 2012, ApJ, 744, L13
Li, X.-D., & van den Heuvel, E. P. J. 1999, ApJ, 513, L45
Lipunov, V. M., Börner, G., & Wadhwa, R. S. 1992, Astrophysics of Neutron Stars (Berlin: Springer)
Lorimer, D. R., Faulkner, A. J., Lyne, A. G., et al. 2006, MNRAS, 372, 777
Manchester, R. N., Hobbs, G. B., Teoh, A., & Hobbs, M. 2005, AJ, 129, 1993
Maraschi, L., & Treves, A. 1981, MNRAS, 194, 1P
Marti, J., & Paredes, J. M. 1995, A&A, 298, 151
McConnell, D., McCulloch, P. M., Hamilton, P. A., et al. 1991, MNRAS, 249, 654
McSwain, M. V., Ray, P. S., Ransom, S. M., et al. 2011, ApJ, 738, 105
Mereghetti, S. 2008, A&AR, 15, 225
Mineshige, S., Rees, M. J., & Fabian, A. C. 1991, MNRAS, 251, 555
Mori, K., & Ruderman, M. A. 2003, ApJ, 592, L75
Okazaki, A. T., Bate, M. R., Ogilvie, G. I., & Pringle, J. E. 2002, MNRAS, 337, 967
Oskinova, L. M., Todt, H., Ignace, R., et al. 2011, MNRAS, 416, 1456
Pacini, F. 1967, Nature, 216, 567
Petit, V., Wade, G. A., Drissen, L., Montmerle, T., & Alecian, E. 2008, MNRAS, 387, L23
Pizzolato, F., Colpi, M., De Luca, A., Mereghetti, S., & Tiengo, A. 2008, ApJ, 681, 530
Popov, S. B., & Turolla, R. 2012, MNRAS, 421, L127
Rea, N., & Esposito, P. 2011, in High-Energy Emission from Pulsars and their Systems, ed. D. F. Torres & N. Rea (Berlin: Springer), 247
Rea, N., Esposito, P., Turolla, R., et al. 2010a, Science, 330, 944
Rea, N., Israel, G. L., Esposito, P., et al. 2012, ApJ, 754, 27
Rea, N., Torres, D. F., van der Klis, M., et al. 2010b, MNRAS, 405, 2206
Reig, P. 2011, Ap&SS, 332, 1
Reig, P., Torrejón, J. M., & Blay, P. 2012, MNRAS, in press (arXiv:1203.1490)
Romero, G. E., Okazaki, A. T., Orellana, M., & Owocki, S. P. 2007, A&A, 474, 15
Shakura, N., Postnov, K., Kochetkova, A., & Hjalmarsdotter, L. 2012, MNRAS, 420, 216
Sierpowska-Bartosik, A., & Torres, D. F. 2008, Astropart. Phys., 30, 239
Spitkovsky, A. 2006, ApJ, 648, L51
Stairs, I. H., Manchester, R. N., Lyne, A. G., et al. 2001, MNRAS, 325, 979
Tavani, M., & Arons, J. 1997, ApJ, 477, 439
Tavani, M., Hermsen, W., van Dijk, R., et al. 1996, A&AS, 120, C243
Torres, D. F., Rea, N., Esposito, P., et al. 2012, ApJ, 744, 106
Torres, D. F., Zhang, S., Li, J., et al. 2010, ApJ, 719, L104
Turolla, R., Zane, S., Pons, J. A., Esposito, P., & Rea, N. 2011, ApJ, 740, 105
van den Heuvel, E. P. J. 2001, in The Neutron Star-Black Hole Connection, ed. C. Kouveliotou, J. Ventura, & E. van den Heuvel (Dordrecht: Kluwer), 173
Wang, N., Johnston, S., & Manchester, R. N. 2004, MNRAS, 351, 599
Wang, Y.-M., & Robertson, J. A. 1985, ApJ, 299, 85
Warner, B. 2003, Cataclysmic Variable Stars (Cambridge: Cambridge Univ. Press)
Waters, L. B. F. M., van den Heuvel, E. P. J., Taylor, A. R., Habets, G. M. H. J., & Persi, P. 1988, A&A, 198, 200
Zabalza, V., Paredes, J. M., & Bosch-Ramon, V. 2011, A&A, 527, A9
Zahn, J.-P. 1977, A&A, 57, 383
Zamanov, R. K. 1995, MNRAS, 272, 308
Zamanov, R. K., Martí, J., Paredes, J. M., et al. 1999, A&A, 351, 543
Zhang, S., Torres, D. F., Li, J., et al. 2010, MNRAS, 408, 642